

Locating quantum critical points with Kibble-Zurek quenches

Michał Białończyk and Bogdan Damski

Jagiellonian University, Institute of Theoretical Physics, Łojasiewicza 11, 30-348 Kraków, Poland
(13/07/2020)

We describe a scheme for finding quantum critical points based on studies of a non-equilibrium susceptibility during continuous quenches taking the system from one phase to another. We assume that two such quenches are performed in opposite directions, and argue that they lead to formation of peaks of a non-equilibrium susceptibility on opposite sides of a critical point. Its position is then narrowed to the interval marked off by these values of the parameter driving the transition, at which the peaks are observed. Universal scaling with the quench time of precision of such an estimation is derived and verified in two exactly solvable models. Experimental relevance of these results and their applicability to localization of classical critical points is expected.

Non-equilibrium phase transitions are ubiquitous in Nature. Their studies, in the context relevant for this work, were started by Kibble, who investigated cosmological phase transitions of the early Universe [1]. It was then proposed by Zurek that similar phenomena can be approached in tabletop condensed matter systems [2]. These theoretical investigations triggered experimental work on non-equilibrium dynamics of superconductors, Josephson junctions, superfluids, ultracold cold atoms and ions, liquid crystals, multiferroics, convective fluids, colloids, etc. Recent surveys of these efforts, discussing dynamics of both classical and quantum phase transitions, can be found in [3–7].

Non-equilibrium dynamics, we are interested in, comes from finite-rate driving of a system across its critical point. Key features of this process are captured by the Kibble-Zurek (KZ) theory, which relates non-equilibrium response of a system to the quench rate and some universal critical exponents.

Phase transitions, however, are also characterized by non-universal (system-specific) properties, among which the position of the critical point clearly stands out. It is the purpose of this work to discuss a simple KZ-related scheme for localization of quantum critical points (Fig. 1). So, we will be dealing with quantum phase transitions [8–10], whose dynamical studies, in the framework of the quantum KZ theory, were initiated by [11–13].

To explain the logic behind our work, we consider some susceptibility χ , whose ground-state value χ^{eq} is algebraically divergent at the critical point g_c , say

$$\begin{aligned}\chi^{eq}(g) &= \chi_{reg}^{eq}(g) + \chi_{sing}^{eq}(g), \\ \chi_{sing}^{eq}(g) &\sim |g - g_c|^{-\gamma}, \quad \gamma > 0,\end{aligned}\quad (1)$$

where the regular (singular) at g_c part of χ^{eq} is denoted as χ_{reg}^{eq} (χ_{sing}^{eq}).

The system will be initially prepared in a ground state far away from the critical point. It will be then quenched towards it by linear in time ramp up of the external parameter driving the transition

$$g(t) = g_c + \frac{t}{\tau_Q}, \quad (2)$$

where inverse of the quench time τ_Q provides the quench rate and the critical point is reached at the time $t_c = 0$.

As long as the system will be far away from the critical point, its evolution will be adiabatic and so its susceptibility will closely match its instantaneous equilibrium value. Near the critical point, however, it cannot be adiabatic because the reaction time of the system, given by the inverse of its energy gap [11], diverges at g_c . So, the susceptibility $\chi(g(t))$ should lag behind $\chi^{eq}(g(t))$. The mismatch between the two will be largest at the critical point, where $\chi(g_c)$, unlike $\chi^{eq}(g_c)$, will be finite (no singularities are expected in the non-equilibrium state of the system, because it will not be given enough time to develop them). Another consequence of the delayed reaction to crossing of the critical point should be seen in the maximum of $\chi(g(t))$, which we expect to appear past the critical point, say at $g_*^\uparrow > g_c$.

Suppose now that the system is initially prepared in a ground state on the other side of the transition, and the parameter $g(t)$ is ramped *down*. The same discussion then leads to the conclusion that $\chi(g(t))$ should have the maximum at some $g_*^\downarrow < g_c$. Therefore, we expect that location of the critical point can be pinned down to the interval $(g_*^\downarrow, g_*^\uparrow)$. This could be of substantial practical relevance, because features such as extrema are typically the easiest to extract from experimental data.

This qualitative description can be made quantitative with the KZ theory, which introduces the characteristic non-equilibrium time scale $\hat{t} \sim \tau_Q^{z\nu/(1+z\nu)}$ and the inter-related field scale

$$\hat{g} = |g(t_c \pm \hat{t}) - g_c| \sim \tau_Q^{-1/(1+z\nu)}, \quad (3)$$

where z and ν are the dynamical and correlation-length universal critical exponents. It can be then argued that near the critical point, the non-equilibrium susceptibility χ will be dominated, for slow-enough quenches, by its universal part

$$\begin{aligned}\chi(g(t)) &\approx \hat{\chi} f\left(\frac{g(t) - g_c}{\hat{g}}\right), \\ \hat{\chi} &= \chi^{eq}[g(t_c \pm \hat{t})] \sim \tau_Q^{\gamma/(1+z\nu)},\end{aligned}\quad (4)$$

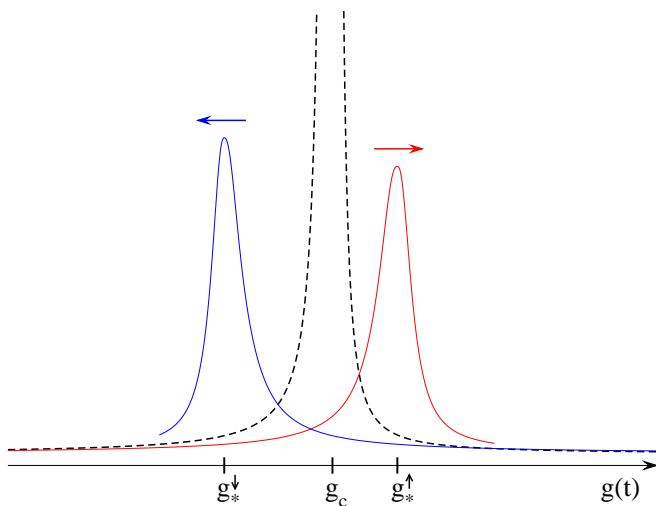


FIG. 1: Schematic plot of our scheme for determination of the critical point. Dashed lines show the equilibrium susceptibility, which is divergent at the critical point g_c . The red (blue) line shows the non-equilibrium susceptibility for the quench, where the parameter g is ramped up (down)–arrows indicate the direction of changes of $g(t)$. The critical point is located between the extrema of these curves, $g_*^\downarrow < g_c < g_*^\uparrow$.

where $f(x)$ is a non-singular scaling function, which is proportional to $|x|^{-\gamma}$ before the onset of non-equilibrium dynamics, so that $\chi(g(t)) \approx \chi_{sing}^{eq}(g(t))$ there. Ansatz (4) combines two basic ingredients of the KZ theory. First, the adiabatic-impulse approximation assuming that system's dynamics is frozen in the impulse regime, i.e. when $|t - t_c| < \hat{t}$, and adiabatic before entering it [11, 14, 15]. This introduces $\hat{\chi}$ into (4). Second, the assumption that non-equilibrium dynamics of physical observables should depend on the rescaled time difference $(t - t_c)/\hat{t}$, which explains the scaling function in (4). The latest take on this ansatz can be found in [16–20], see e.g. [21] for preceding work in the context of classical phase transitions.

It now follows from (4) that precision of critical point determination should increase with the quench time as

$$\delta = g_*^\uparrow - g_*^\downarrow \sim \tau_Q^{-1/(1+z\nu)}, \quad (5)$$

which is of interest from the metrological perspective (the KZ theory has been only recently explored in the metrological context [22]). Eq. (5) can be also used for extracting the product of universal critical exponents from experimental data. We also mention that susceptibilities, to the best of our knowledge, were studied in the KZ context only in [23, 24]. Finally, it is perhaps worth to say that our approach does not specify, where the critical point is located within the $(g_*^\downarrow, g_*^\uparrow)$ interval (we have checked that it is there in all our simulations). Two exactly solvable models will be used below for illustration of above-introduced concepts (their numerical solutions will be presented on Figs. 2–7, see [25] for technical details).

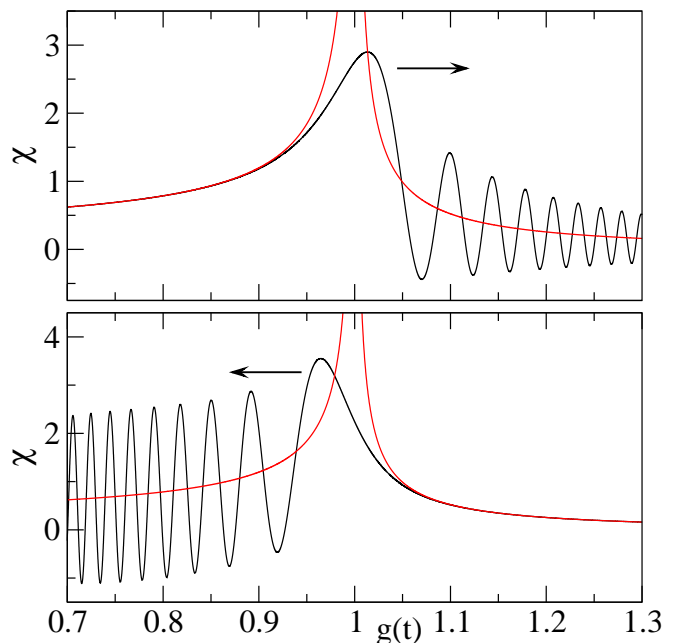


FIG. 2: Dynamics of the susceptibility $\chi(g(t))$ during up and down quenches in the extended XY model is presented by black lines in upper and lower panels, respectively. The instantaneous equilibrium value of the susceptibility, $\chi^{eq}(g(t))$, is provided by red lines. The quench time $\tau_Q = 300$.

Extended XY model. We take the Hamiltonian

$$H = - \sum_{i=1}^N (\sigma_i^x \sigma_{i+1}^x + \frac{1}{3} \sigma_i^y \sigma_{i+1}^y - \frac{1}{3} \sigma_i^x \sigma_{i+1}^z \sigma_{i+2}^x + g \sigma_i^z), \quad (6)$$

where $g \geq 0$ is the external magnetic field, $\sigma_i^{x,y,z}$ are Pauli matrices acting on the i -th spin, N is the number of spins, and periodic boundary conditions are implemented. Basic properties of this model were described in [19, 26]. Its critical point is at $g_c = 1$ and it separates ferromagnetic ($0 < g < 1$) and paramagnetic ($g > 1$) phases. Critical exponents of (6) are $z = 3$ and $\nu = 1/3$.

As the susceptibility of interest in our translationally-invariant system, we take derivative of the transverse magnetization at an arbitrary lattice site

$$\chi = \frac{d\langle \sigma_i^z \rangle}{dg}. \quad (7)$$

In equilibrium, this quantity is algebraically divergent at the critical point. Indeed, $\chi^{eq} = -d^2 E_0 / dg^2$ from the Feynman-Hellmann theorem, where E_0 is the ground state energy per lattice site. The singular part of E_0 is typically assumed to scale as $|g - g_c|^{2-\alpha}$. If we now combine this insight with the quantum hyperscaling relation—i.e. $\alpha = 2 - \nu(d + z)$, where d represents system dimensionality [9]—we will get that $\alpha = 2/3$ for model (6). Thus, $\chi_{sing}^{eq}(g)$ is given by (1) with $g_c = 1$ and $\gamma = 2/3$, which we have numerically verified, and so $\hat{\chi} \sim \tau_Q^{1/3}$.

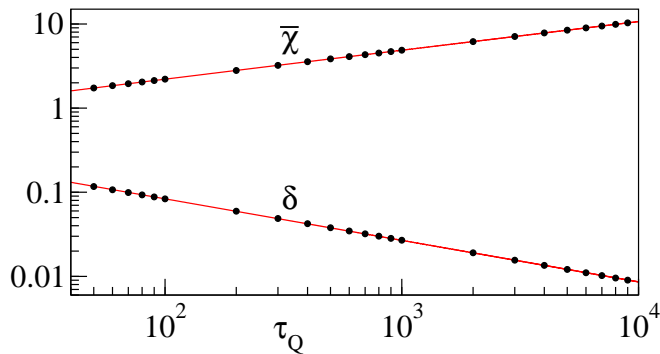


FIG. 3: Global maxima of the non-equilibrium susceptibility χ of the extended XY model. Upper data: the average value of χ at global maxima during up and down quenches. Lower data: the distance δ between such maxima. Red lines show fits to black dots coming from numerics, see (10) and (11).

The ramp up of the magnetic field will be done with

$$g(t) = \left(\frac{t}{2\tau_Q}\right)^2, \quad (8)$$

while its ramp down will be done with

$$g(t) = g_0 - \frac{t}{\tau_Q}, \quad g_0 = 5. \quad (9)$$

Both quenches start from ground states at $t = 0$ and then the system is driven towards the critical point, which is reached at t_c equal to $2\tau_Q$ and $(g_0 - 1)\tau_Q$ for up (8) and down (9) quenches, respectively.

These quenches share the same important property. Namely, their rate, given by $|dg/dt|$, is equal to τ_Q^{-1} at t_c . Thus, near the critical point, the driving proceeds just as in model quench (2), which is all that should matter in the context of the KZ theory (see e.g. [27] for a similar quadratic-in-time quench studied in the KZ framework).

As for differences between (8) and (9), we note that quenches typically produce excitations at the beginning of time evolution (see e.g. [24]). Such excitations are of no interest in our studies. They appear because variations of the external parameter are not smoothly turned on (the more low-order derivatives of the external parameter vanish at $t = 0$, the more adiabatic the quench initially is). Quadratic time dependence in (8) noticeably reduces initial excitation of our system with respect to what would happen if the up quench would be linear. The situation is somewhat similar for down quenches (9). However, the gap in the excitation spectrum is much larger at $g_0 \gg 1$ than at $g = 0$. Even for linear quenches, we find that it sufficiently reduces initial non-adiabaticity of our observable during “down” evolutions (the same happens in the Ising model studied below).

Typical dynamics of susceptibility (7) is presented in Fig. 2, where we see three distinct regimes. First, the evolution is adiabatic. Then, near the critical point, the

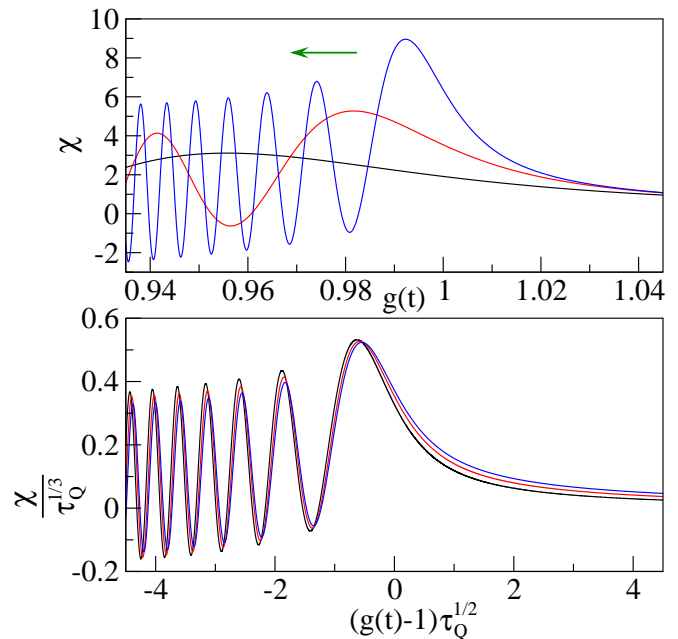


FIG. 4: Dynamics of the susceptibility χ during down quenches of the extended XY model. Black, red, and blue lines are obtained for $\tau_Q = 200, 1000,$ and 5000 , respectively. Panels show results before and after KZ rescalings.

susceptibility lags behind its instantaneous equilibrium value, and a well visible global maximum appears after crossing the critical point. Finally, the susceptibility oscillates, which can be regarded as a quasi-adiabatic stage (no more excitations are generated, system’s dynamics revolves around the instantaneous equilibrium solution).

More quantitatively, from numerical data presented in Fig. 3, we find that the distance δ between global maxima for up and down quenches is described by

$$\ln \delta = -0.209(3) - 0.4936(5) \ln \tau_Q. \quad (10)$$

This result comes from a linear regression [28]. It is in excellent agreement with (5) suggesting a prefactor of $-1/2$ in front of the logarithm.

It is also instructive to have a look at the average value of the susceptibility at global maxima, which we denote by χ_*^\uparrow and χ_*^\downarrow for up and down quenches, respectively. The nonlinear fit to data from Fig. 3 shows that

$$\bar{\chi} = (\chi_*^\uparrow + \chi_*^\downarrow)/2 = -0.063(2) + 0.4795(7)\tau_Q^{0.3376(2)}, \quad (11)$$

where the exponent is in excellent agreement with the value of $1/3$ due to $\gamma = 2/3$ and $z\nu = 1$ (4). Finally, we verify ansatz (4) in Fig. 4, where good overlap between non-equilibrium susceptibilities, obtained for vastly different quench times τ_Q , is seen after proper rescalings.

Ising model. The Hamiltonian of interest now is

$$H = - \sum_{i=1}^N (\sigma_i^x \sigma_{i+1}^x + g \sigma_i^z), \quad (12)$$

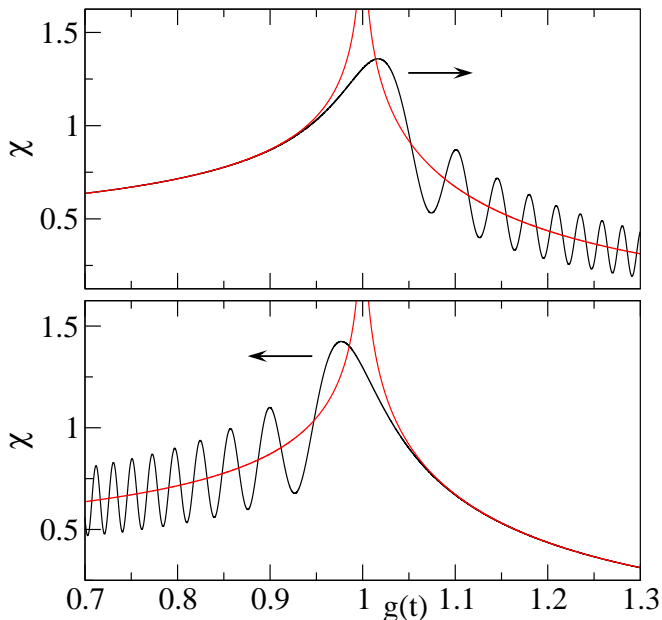


FIG. 5: Black lines: the susceptibility $\chi(g(t))$ during up (upper panel) and down (lower panel) quenches of the Ising model with $\tau_Q = 300$. Red lines: the equilibrium value of χ .

where the critical point and phases are the same as in the extended XY chain [29–31]. Dynamics of this paradigmatic model, under continuous driving such as (2), was studied in [12, 13, 16, 18, 24, 32–46]. Key differences between (6) and (12) are seen through critical exponents, which are now given by $z = \nu = 1$.

Such values lead to non-algebraic singularity of the equilibrium version of susceptibility (7), which can be understood by noting that $\alpha = 0$ now. Indeed, χ_{sing}^{eq} has the following expansion near the critical point [23]

$$\chi_{sing}^{eq}(g) \approx -\frac{1}{\pi} \ln |g - 1|. \quad (13)$$

This well-known result is a bit unusual because one typically expects algebraic singularities as in (1). It has interesting consequences on χ , whose scaling properties are not captured by (4). The appropriate KZ ansatz reads

$$\chi(g(t)) \approx f\left(\frac{g(t) - g_c}{\hat{g}}\right) + \frac{\ln \tau_Q}{2\pi}, \quad (14)$$

where up to a constant term, $f(x)$ is approximated by $-\frac{1}{\pi} \ln |x|$ before the onset of non-equilibrium dynamics. To get (14), one can start with $d^2 \langle \sigma_i^z \rangle / dg^2$, whose equilibrium value is algebraically divergent at the critical point, apply ansatz (4) to it, integrate the resulting expression, and take into account adiabaticity before the beginning of non-equilibrium dynamics [25]. Alternatively, one may adopt results from [23], where $d \langle \sigma_i^z \rangle / dg$ was studied with renormalization group techniques in a time-independent but spatially inhomogeneous Ising chain. This is done by replacing λ_Q with τ_Q in Eq. (26) from [23].

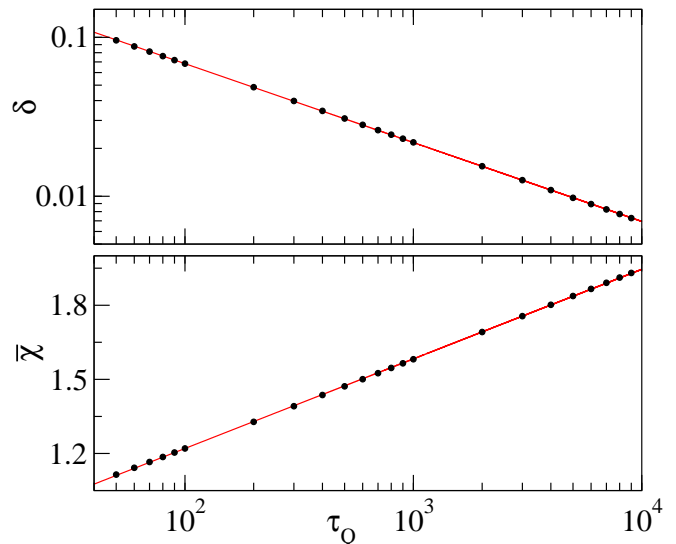


FIG. 6: Upper panel: the distance δ between global maxima of the susceptibility χ appearing during up and down quenches of the Ising model. Lower panel: arithmetic average of the value of χ at those maxima. Black dots show numerics, red lines are fits (15) and (16).

Typical dynamics of the susceptibility χ , due to either (8) or (9), is shown in Fig. 5. The fits from Fig. 6 are

$$\ln \delta = -0.397(3) - 0.4965(4) \ln \tau_Q, \quad (15)$$

$$\bar{\chi} = 0.495(2) + 0.1575(2) \ln \tau_Q, \quad (16)$$

which can be compared to our theory. The prefactor in front of the logarithm in (15) should be $-1/2$, and indeed it is very much so. The one in (16) is also very close to our expectations, i.e. $1/2\pi \approx 0.159$ due to (14). Finally, verification of ansatz (14) is shown in Fig. 7, where pretty good overlap between curves is found.

Summarizing, we have proposed how quantum critical points can be accurately localized by scanning a non-equilibrium susceptibility during Kibble-Zurek quenches. Our scheme assumes that two such scans are performed by either increasing or decreasing the external parameter driving the transition. We have argued that each of them should lead to formation of a peak of a non-equilibrium susceptibility, and that the critical point can be pinned down to the interval marked off by these values of the external parameter, at which the peaks are observed. The width of such an interval has been argued to exhibit universal power-law scaling with the quench time, shrinking to zero in the adiabatic limit.

We have tested these predictions in two exactly solvable models, exhibiting either algebraic or logarithmic singularities of equilibrium susceptibilities. We have found that each quench actually produces a train of progressively smaller susceptibility peaks. By focusing on the highest one for each quench, our expectations have been precisely confirmed.

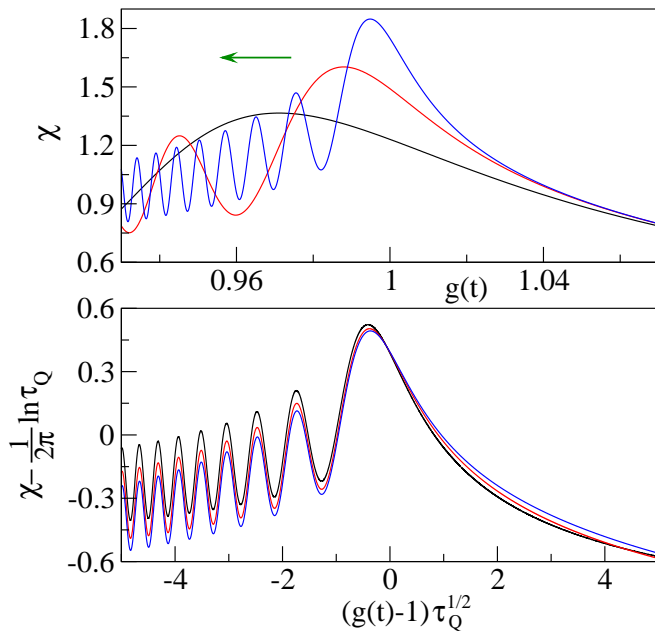


FIG. 7: Dynamics of the susceptibility χ during down quenches of the Ising model: before and after KZ rescalings motivated by ansatz (14). Black, red, and blue lines are numerically obtained for $\tau_Q = 200, 1000, \text{ and } 5000$.

There are several prospective extensions of these studies. First, similar calculations can be done in other models, which should increase our understanding of their dynamics. Second, our predictions can be used for experimental determination of phase diagrams of physical systems through their non-equilibrium response to variations of external fields [47]. In particular, one should be able to readily implement our scheme in cold atom and ion emulators of spin systems [48–52], whose dynamical experimental studies were recently reported in [53–56]. Finally, we expect that the same scheme can be applied for localization of classical critical points, because the Kibble-Zurek theory similarly describes dynamics of quantum and classical systems [3–7]. This should open the door for experimental tests of our scheme in various setups listed at the very beginning of this work.

We thank Adolfo del Campo for a remark triggering our interest in this subject and for his comments about the manuscript. We also thank Marek Rams for discussions of the extended XY model and his remarks about the manuscript. MB and BD were supported by the Polish National Science Centre (NCN) grant DEC-2016/23/B/ST3/01152.

[1] T. W. B. Kibble, *Phys. Rep.* **67**, 183 (1980).
 [2] W. H. Zurek, *Phys. Rep.* **276**, 177 (1996).
 [3] T. Kibble, *Phys. Today* **60**, 47 (2007).

[4] J. Dziarmaga, *Adv. Phys.* **59**, 1063 (2010).
 [5] A. Polkovnikov, K. Sengupta, A. Silva, and M. Vengalattore, *Rev. Mod. Phys.* **83**, 863 (2011).
 [6] A. del Campo, T. W. B. Kibble, and W. H. Zurek, *J. Phys.: Condens. Matter* **25**, 404210 (2013).
 [7] A. del Campo and W. H. Zurek, *Int. J. Mod. Phys. A* **29**, 1430018 (2014).
 [8] S. Sachdev *Quantum Phase Transitions* (Cambridge University Press, 2011).
 [9] M. Continentino *Quantum Scaling in Many-Body Systems: An Approach to Quantum Phase Transitions* (Cambridge University Press, 2nd edition, 2017).
 [10] S. Sachdev and B. Keimer, *Phys. Today* **64**, 29 (2011).
 [11] B. Damski, *Phys. Rev. Lett.* **95**, 035701 (2005).
 [12] W. H. Zurek, U. Dorner, and P. Zoller, *Phys. Rev. Lett.* **95**, 105701 (2005).
 [13] J. Dziarmaga, *Phys. Rev. Lett.* **95**, 245701 (2005).
 [14] B. Damski and W. H. Zurek, *Phys. Rev. A* **73**, 063405 (2006).
 [15] M. Tomka, L. Campos Venuti, and P. Zanardi, *Phys. Rev. A* **97**, 032121 (2018).
 [16] M. Kolodrubetz, B. K. Clark, and D. A. Huse, *Phys. Rev. Lett.* **109**, 015701 (2012).
 [17] A. Chandran, A. Erez, S. S. Gubser, and S. L. Sondhi, *Phys. Rev. B* **86**, 064304 (2012).
 [18] A. Francuz, J. Dziarmaga, B. Gardas, and W. H. Zurek, *Phys. Rev. B* **93**, 075134 (2016).
 [19] D. Sadhukhan, A. Sinha, A. Francuz, J. Stefaniak, M. M. Rams, J. Dziarmaga, and W. H. Zurek, *Phys. Rev. B* **101**, 144429 (2020).
 [20] D. Rossini and E. Vicari, *Phys. Rev. Research* **2**, 023211 (2020).
 [21] B. Damski and W. H. Zurek, *Phys. Rev. Lett.* **104**, 160404 (2010).
 [22] M. M. Rams, P. Sierant, O. Dutta, P. Horodecki, and J. Zakrzewski, *Phys. Rev. X* **8**, 021022 (2018).
 [23] M. Łącki and B. Damski, *J. Stat. Mech.* (2017) 103105.
 [24] M. M. Rams, J. Dziarmaga, and W. H. Zurek, *Phys. Rev. Lett.* **123**, 130603 (2019).
 [25] Supplemental Material attached to this manuscript.
 [26] M. Suzuki, *Prog. Theor. Phys.* **46**, 1337 (1971).
 [27] B. Damski and W. H. Zurek, *New J. Phys.* **10**, 045023 (2008).
 [28] One standard error, delivered by NonlinearModelFit function from [57], is provided in brackets in all our fitting results.
 [29] E. Lieb, T. Schultz, and D. Mattis, *Ann. Phys. (N.Y.)* **16**, 407 (1961).
 [30] P. Pfeuty, *Ann. Phys.* **57**, 79 (1970).
 [31] B. Damski and M. M. Rams, *J. Phys. A* **47**, 025303 (2014).
 [32] A. Polkovnikov, *Phys. Rev. B* **72**, 161201(R) (2005).
 [33] S. Mostame, G. Schaller, and R. Schützhold, *Phys. Rev. A* **76**, 030304(R) (2007).
 [34] R. Barankov and A. Polkovnikov, *Phys. Rev. Lett.* **101**, 076801 (2008).
 [35] S. Mondal, K. Sengupta, and D. Sen, *Phys. Rev. B* **79**, 045128 (2009).
 [36] D. Patanè, L. Amico, A. Silva, R. Fazio, and G. E. Santoro, *Phys. Rev. B* **80**, 024302 (2009).
 [37] L. Cincio, J. Dziarmaga, M. M. Rams, and W. H. Zurek, *Phys. Rev. A* **75**, 052321 (2007).
 [38] K. Sengupta and D. Sen, *Phys. Rev. A* **80**, 032304 (2009).
 [39] A. Das, *Phys. Rev. B* **82**, 172402 (2010).

- [40] A. Russomanno, S. Sharma, A. Dutta, and G. E. Santoro, *J. Stat. Mech.* (2015) P08030.
- [41] B. Damski, Fidelity approach to quantum phase transitions in quantum Ising model, in *Quantum Criticality in Condensed Matter: Phenomena, Materials and Ideas in Theory and Experiment*, edited by J. Jędrzejewski (World Scientific, Singapore, 2015), pp. 159–182; arXiv:1509.03051.
- [42] T. Puskarov and D. Schuricht, *SciPost Phys.* **1**, 003 (2016).
- [43] S. Lorenzo, J. Marino, F. Plastina, G. M. Palma, and T. J. G. Apollaro, *Sci. Rep.* **7**, 5672 (2017).
- [44] M. Białończyk and B. Damski, *J. Stat. Mech.* (2018) 073105.
- [45] A. del Campo, *Phys. Rev. Lett.* **121**, 200601 (2018).
- [46] M. Białończyk and B. Damski, *J. Stat. Mech.* (2020) 013108.
- [47] If determination of a non-equilibrium susceptibility would require differentiation of noisy data, one may need to smooth such data first. This can be done with various techniques, see e.g. [58] for the Padé approximant approach.
- [48] D. Porras and J. I. Cirac, *Phys. Rev. Lett.* **92**, 207901 (2004).
- [49] S. Korenblit *et al.*, *New J. Phys.* **14**, 095024 (2012).
- [50] M. Lewenstein, A. Sanpera, V. Ahufinger, B. Damski, A. Sen De, and U. Sen, *Adv. Phys.* **56**, 243 (2007).
- [51] C. Gross and I. Bloch, *Science* **357**, 995 (2017).
- [52] P. Schauss, *Quantum Sci. Technol.* **3**, 023001 (2018).
- [53] H. Bernien *et al.*, *Nature* **551**, 579 (2017).
- [54] J. Zhang, G. Pagano, P. W. Hess, A. Kyprianidis, P. Becker, H. Kaplan, A. V. Gorshkov, Z.-X. Gong, and C. Monroe, *Nature* **551**, 601 (2017).
- [55] A. Keesling *et al.*, *Nature* **568**, 207 (2019).
- [56] V. Makhalov, T. Satoor, A. Evrard, T. Chalopin, R. Lopes, and S. Nascimbene, *Phys. Rev. Lett.* **123**, 120601 (2019).
- [57] Wolfram Research, Inc., *Mathematica*, Version 12.0, Champaign, IL (2019).
- [58] O. A. Prośniak, M. Łącki, and B. Damski, *Sci. Rep.* **9**, 8687 (2019).

–Supplemental Material–
Locating quantum critical points with Kibble-Zurek quenches

Michał Białończyk and Bogdan Damski
Jagiellonian University, Institute of Theoretical Physics, Łojasiewicza 11, 30-348 Kraków, Poland

Contents

I. Numerical simulations of the Ising model	1
II. Numerical simulations of the extended XY model	2
III. The scaling ansatz for the susceptibility of the Ising model	3

I. NUMERICAL SIMULATIONS OF THE ISING MODEL

In the main text, we have introduced the periodic Ising Hamiltonian

$$H = - \sum_{i=1}^N (\sigma_i^x \sigma_{i+1}^x + g \sigma_i^z). \quad (\text{S1})$$

The model defined by (S1) is conveniently discussed by mapping spins onto non-interacting fermions via the Jordan-Wigner transformation

$$\sigma_i^z = 1 - 2c_i^\dagger c_i, \quad \sigma_i^x = (c_i + c_i^\dagger) \prod_{j<i} (1 - 2c_j^\dagger c_j), \quad \{c_i, c_j^\dagger\} = \delta_{ij}, \quad \{c_i, c_j\} = 0. \quad (\text{S2})$$

A careful analysis then shows that anti-periodic boundary conditions have to be imposed on fermionic operators c_i , if our system is composed of an even number of spins and we start time evolution from its ground state [S1, S2]. Both conditions are satisfied in our numerical simulations.

One then goes to the momentum space through the substitution

$$c_j = \frac{\exp(-i\pi/4)}{\sqrt{N}} \sum_{K=\pm k} c_K \exp(iKj), \quad k = \frac{\pi}{N}, \frac{3\pi}{N}, \dots, \pi - \frac{\pi}{N}, \quad (\text{S3})$$

arriving at

$$H = 2 \sum_k \left[(c_k^\dagger c_k - c_{-k} c_{-k}^\dagger) (g - \cos k) + (c_k^\dagger c_{-k}^\dagger + c_{-k} c_k) \sin k \right], \quad (\text{S4})$$

which can be diagonalized via the Bogolubov transformation. The ground state of (S4) is

$$|g\rangle = \prod_k (u_k^{eq} - v_k^{eq} c_k^\dagger c_{-k}^\dagger) |\text{vac}\rangle, \quad (\text{S5})$$

$$u_k^{eq} = \cos \frac{\theta_k}{2}, \quad v_k^{eq} = \sin \frac{\theta_k}{2}, \quad (\text{S6})$$

$$\sin \theta_k = \frac{\sin k}{\sqrt{g^2 - 2g \cos k + 1}}, \quad \cos \theta_k = \frac{g - \cos k}{\sqrt{g^2 - 2g \cos k + 1}}, \quad (\text{S7})$$

where the vacuum state $|\text{vac}\rangle$ is annihilated by all $c_{\pm k}$ operators.

From the time-dependent Schrödinger equation,

$$i \frac{d}{dt} |\psi(t)\rangle = H[g(t)] |\psi(t)\rangle, \quad (\text{S8})$$

one then finds that [S1]

$$|\psi(t)\rangle = \prod_k (u_k(t) - v_k(t)c_k^\dagger c_{-k}^\dagger) |\text{vac}\rangle, \quad (\text{S9})$$

$$i \frac{d}{dt} \begin{pmatrix} v_k \\ u_k \end{pmatrix} = 2 \begin{pmatrix} g(t) - \cos k & -\sin k \\ -\sin k & \cos k - g(t) \end{pmatrix} \begin{pmatrix} v_k \\ u_k \end{pmatrix}. \quad (\text{S10})$$

The above differential equations are efficiently numerically solved with standard techniques. The initial conditions are chosen such that u_k and v_k , at the beginning of time evolution, are equal to u_k^{eq} and v_k^{eq} , respectively. The latter are computed at the initial value of the magnetic field.

The non-equilibrium transverse magnetization is given by

$$S^z(g(t)) = \langle \psi(t) | \sigma_i^z | \psi(t) \rangle = 1 - \frac{4}{N} \sum_k |v_k(t)|^2. \quad (\text{S11})$$

Its equilibrium value is obtained after the replacements $|\psi(t)\rangle \rightarrow |g\rangle$ and $v_k(t) \rightarrow v_k^{eq}$. From (S11), the non-equilibrium susceptibility χ is numerically computed via

$$\chi(g_{i+1/2}) = \chi \left(g_i + \frac{g_{i+1} - g_i}{2} \right) \approx \frac{S^z(g_{i+1}) - S^z(g_i)}{g_{i+1} - g_i}, \quad g_i = g(t_i). \quad (\text{S12})$$

The grid, which we use for computation of this quantity, is $g_{i+1} - g_i = 5 \cdot 10^{-5}$. The equilibrium susceptibility χ^{eq} is trivially computed through analytic differentiation.

We identify positions of maxima of the non-equilibrium susceptibility in the following way. First, we choose τ_Q and find the maximum on the susceptibility vs. magnetic field plot, say at $(g_{j+1/2}, \chi(g_{j+1/2}))$. We then fit a parabola to the points $(g_{i+1/2}, \chi(g_{i+1/2}))$ around it, satisfying $\chi(g_{i+1/2}) \geq \chi(g_{j+1/2})(1 - \epsilon)$, where $\epsilon = 0.0025$ is chosen (the twice larger ϵ gives essentially identical results). The maximum of such obtained parabola is then analyzed in the main text. The fitting procedure makes our results independent of tiny oscillations of data points. It also allows for interpolation of positions of maxima between the grid points.

Our numerics, presented in the main text, have been done for systems composed of $N = 2000$ spins. This imposes an upper limit on quench times, for which Kibble-Zurek dynamics should be free from finite-size effects. Namely, the size of the system should be much larger than the correlation length around the time, when the system goes out of equilibrium [S3]. The latter is proportional to $\tau_Q^{\nu/(1+z\nu)}$ [S3, S4]. So, this condition leads to $\tau_Q \ll N^2$ in the Ising chain, which is satisfied in all our numerical simulations. In accordance with these expectations, we have directly verified that virtually identical results, to those reported in the main text, are also obtained when $N = 1000$. Finally, in the main text, we do the fits to numerics in the range $50 \leq \tau_Q \leq 9000$.

II. NUMERICAL SIMULATIONS OF THE EXTENDED XY MODEL

In the main text, we have introduced the Hamiltonian of the periodic extended XY model

$$H = - \sum_{i=1}^N (\sigma_i^x \sigma_{i+1}^x + \frac{1}{3} \sigma_i^y \sigma_{i+1}^y - \frac{1}{3} \sigma_i^x \sigma_{i+1}^z \sigma_{i+2}^x + g \sigma_i^z). \quad (\text{S13})$$

This model is solved with the help of (S2) supplemented by $\sigma_i^y = i(c_i^\dagger - c_i) \prod_{j<i} (1 - 2c_j^\dagger c_j)$.

As is explained in [S5], all the steps that have to be performed, for diagonalization and time-evolution of the model defined by (S13), are completely analogical to those discussed in Sec. I. The only differences are that (S4), (S7), and (S10) get replaced by

$$H = 2 \sum_k \left[(c_k^\dagger c_k - c_{-k} c_{-k}^\dagger) \left(g - \frac{4}{3} \cos k + \frac{1}{3} \cos 2k \right) + (c_k^\dagger c_{-k}^\dagger + c_{-k} c_k) \left(\frac{2}{3} \sin k - \frac{1}{3} \sin 2k \right) \right], \quad (\text{S14})$$

$$\begin{aligned} \sin \theta_k &= \frac{\frac{2}{3} \sin k - \frac{1}{3} \sin 2k}{\sqrt{\left(g - \frac{4}{3} \cos k + \frac{1}{3} \cos 2k \right)^2 + \left(\frac{2}{3} \sin k - \frac{1}{3} \sin 2k \right)^2}}, \\ \cos \theta_k &= \frac{g - \frac{4}{3} \cos k + \frac{1}{3} \cos 2k}{\sqrt{\left(g - \frac{4}{3} \cos k + \frac{1}{3} \cos 2k \right)^2 + \left(\frac{2}{3} \sin k - \frac{1}{3} \sin 2k \right)^2}}, \end{aligned} \quad (\text{S15})$$

and

$$i \frac{d}{dt} \begin{pmatrix} v_k \\ u_k \end{pmatrix} = 2 \begin{pmatrix} g(t) - \frac{4}{3} \cos k + \frac{1}{3} \cos 2k & \frac{1}{3} \sin 2k - \frac{2}{3} \sin k \\ \frac{1}{3} \sin 2k - \frac{2}{3} \sin k & -g(t) + \frac{4}{3} \cos k - \frac{1}{3} \cos 2k \end{pmatrix} \begin{pmatrix} v_k \\ u_k \end{pmatrix}, \quad (\text{S16})$$

respectively. We mention in passing that there are misprints in the expression for (S14) in [S5].

Almost all remarks from Sec. I, which are below (S10), also describe our studies of the extended XY model. The only difference is that the condition for finite-size-independence of KZ dynamics now reads $\tau_Q \ll N^6$, because $z = 3$ and $\nu = 1/3$ in this model [S5].

III. THE SCALING ANSATZ FOR THE SUSCEPTIBILITY OF THE ISING MODEL

To support the scaling ansatz for the susceptibility χ of the Ising model, we start from consideration of

$$\tilde{\chi} = \frac{d\chi}{dg}. \quad (\text{S17})$$

Its equilibrium singular part is given by

$$\tilde{\chi}_{sing}^{eq} \approx \frac{1}{\pi(1-g)}, \quad (\text{S18})$$

and so $\tilde{\chi}^{eq}$ is algebraically divergent at the critical point. Applying to (S17) scaling ansatz (4) from the main text, we get

$$\tilde{\chi} \approx \sqrt{\tau_Q} \tilde{f}((g-1)\sqrt{\tau_Q}), \quad (\text{S19})$$

which, when combined with (S17), leads to

$$\frac{d\chi}{dx} \approx \tilde{f}(x), \quad x = (g-1)\sqrt{\tau_Q}. \quad (\text{S20})$$

Integrating (S20) over x , we get

$$\chi \approx h(x) + C, \quad (\text{S21})$$

where h is a new scaling function. To fix the x -independent C term, we require that $\chi(x \ll -1)$ for the up quench and $\chi(x \gg 1)$ for the down quench are well-approximated by

$$\chi_{sing}^{eq} \approx -\frac{1}{\pi} \ln |g-1|. \quad (\text{S22})$$

Then, we note that by definition scaling functions can depend on τ_Q only through their argument. This leads to the conclusion that

$$\chi \approx h((g-1)\sqrt{\tau_Q}) + \frac{\ln \tau_Q}{2\pi}, \quad (\text{S23})$$

where $h(x \ll -1)$ for the up quench and $h(x \gg 1)$ for the down quench are well-approximated by $-\frac{1}{\pi} \ln |x|$. After identification of $h((g-1)\sqrt{\tau_Q})$ with $f((g(t)-g_c)/\hat{g})$, (S23) matches the expression from the main text. We mention in passing that a factor of 2, in the denominator of the second term in (S23), can be traced back to $1+z\nu=2$.

[S1] J. Dziarmaga, Phys. Rev. Lett. **95**, 245701 (2005).

[S2] B. Damski and M. M. Rams, J. Phys. A **47**, 025303 (2014).

[S3] J. Dziarmaga, Adv. Phys. **59**, 1063 (2010).

[S4] W. H. Zurek, U. Dorner, and P. Zoller, Phys. Rev. Lett. **95**, 105701 (2005).

[S5] D. Sadhukhan, A. Sinha, A. Francuz, J. Stefaniak, M. M. Rams, J. Dziarmaga, and W. H. Zurek, Phys. Rev. B **101**, 144429 (2020).